RGNZ/MGPB

Three-Dimensional Seepage Back Analysis of Dam Foundation and Abutments: a Case Study of the Karkheh Dam

Rudarsko-geološko-naftni zbornik
(The Mining-Geology-Petroleum Engineering Bulletin)
DOI: 10.17794/rgn.2026.4.5

Original scientific paper

Mohammad Salehinik[1], AliAsghar Mirghasemi[2]*, Ahmadreza Tabibnejad[3]
[1,2] *School of Civil Engineering, College of Engineering, University of Tehran, Tehran, Iran.*
[3] *Mahab Ghods Consulting Engineer, Takharestan St., Zafar St., Tehran, Iran.*

Abstract
The foundation of the Karkheh Dam comprises a heterogeneous geological profile of highly permeable conglomerate layers interbedded with relatively impervious mudstones. Following the extreme flood events of March and April 2019, the reservoir first reached its normal water level (NWL) of 220 m above sea level and subsequently rose by approximately 5 m, peaking at 224.82 m on April 5. Although the dam crest is at 234 m, these conditions raised concerns regarding structural stability and potential seepage hazards, particularly during future floods. To mitigate these risks, strict operational measures were implemented to limit the hydraulic gradient within allowable design values, thereby reducing the likelihood of internal erosion and piping in the foundation and abutments. A three-dimensional seepage model of the foundation and abutment system was developed using FEFLOW 3D, incorporating six conglomerate layers at four reservoir levels. The model was calibrated against monitored seepage discharges by adjusting hydraulic conductivity coefficients and validated with piezometric data. The key results included the identification of the uplift pressure distribution beneath the spillway chute and pinpointing the location of maximum uplift pressure, which is critical for implementing new drainage wells. In addition, the analyses determined a threshold reservoir elevation above which the maximum average hydraulic gradient increases to levels that pose a heightened risk of internal erosion in the foundation and abutments. These findings, along with refined permeability parameters and hydraulic gradient distributions, provide deeper insight into the dam's hydro-geotechnical response under extreme hydrological loading and support targeted hydraulic safety management.

Keywords:
Seepage Analysis; Earth Dam; Hydraulic Gradient; Dam Monitoring; FEFLOW3D

1. Introduction

Seepage, defined as the gradual migration of water through soil or rock media, plays a pivotal role in the safety and long-term performance of embankment dams. Globally, earth dams remain susceptible to three principal modes of failure: external erosion from overtopping, internal erosion including piping and suffusion, and slope instability (**Foster et al., 2000**). Ensuring slope stability and controlling hydraulic behaviour within seepage-control elements are central to dam safety management. However, existing research reveals a noticeable gap in the systematic evaluation of embankment dam slope stability with respect to hydraulic control parameters, particularly under coupled seepage–stress conditions and fluctuating reservoir water levels (**Zhou et al., 2023**). Understanding the mechanisms by which internal erosion develops is essential for explaining how seepage-induced failure initiates and progresses in embankment dams. Important studies have advanced understanding of internal erosion mechanisms. Experimental relationships between limit curves and critical hydraulic gradients for piping in sandy gravels have been established (**Skempton & Brogan, 1994**). Similarly, experimental results on hydraulic gradients for various materials have been presented (**Choe et al., 2022**). Literature has addressed the need for an integrated definition of the critical hydraulic gradient that incorporates stress state effects. Experimental tests on a poorly graded mixture of washed Leighton Buzzard sand and decomposed granite, with a gap ratio indicative of internal stability, showed that the hydraulic gradient initiating erosion (i_{statrt}) increased from 0.7 to 1.77 as mean stress rose from 10 kPa to 200 kPa, due to reduced porosity (**Chang & Zhang, 2013**). Furthermore, microscopic observations of their study revealed that pore structure evolution strongly influences hydraulic gradients, with changes in connectivity affecting erosion potential. Loss of fine particles disrupts force chains, sharply increasing susceptibility to erosion. These effects mainly act during the linear

* Corresponding author: Ali Asghar Mirghasemi
e-mail address: aghasemi@ut.ac.ir
Received: 7 September 2025. Accepted: 26 January 2026.
Available online: 21 July 2026

compression phase of the soil's stress–strain response, indicating that the initial stress state is a key factor governing permeability (**Zhang et al., 2022**). For instance, a review of methods to determine conductivity in fractured rock masses noted that normal stress tends to reduce permeability, while shear stress may increase it (**Shahbazi et al., 2020**). While these physical processes are now better understood, predicting their occurrence in practice requires accounting for the natural variability and uncertainty of soil hydraulic properties.

Since seepage parameters are inherently non-deterministic, their treatment as random variables has been explored (**Shahbazi et al., 2020; Zhang et al., 2022**). Several studies have employed spatially variable random fields to account for heterogeneity in geotechnical parameters (**Zhou et al., 2024**). Seepage parameter inversion for earth-rockfill dams has been implemented using an Improved Chaos Sparrow Search Algorithm (ICSSA) combined with a radial basis function (RBF) neural network (**Zhou et al., 2024**). Seepage parameters can be calibrated using seepage monitoring data. Numerical simulations employing these calibrated parameters would produce more realistic and accurate results. Typical calibration methods for geotechnical parameters are detailed in literature (**Xuefeng et al., 2019**). Calibration against monitoring data, particularly from observation wells, enhances the realism of numerical simulations (**Ganjalipour & Fatemi Aghda, 2019**). Back-analysis methods, such as minimising the weighted sum of squared deviations between calculated and observed heads, are effective for optimizing permeability parameters (**Ren et al., 2016**). Building upon these uncertainty-based approaches, recent developments in numerical and artificial intelligence techniques have advanced the accuracy and scope of seepage analysis.

A variety of approaches exist for seepage analysis (**Al-Janabi et al., 2025**). In recent years, Artificial Intelligence techniques, such as feed forward neural networks, support vector regression, and adaptive neuro fuzzy inference systems have been increasingly applied to improve the predictive accuracy of piezometric head measurements, as demonstrated through seepage modelling of the Sattarkhan earth fill dam in northwestern Iran (**Sharghi et al., 2018**). More recently, Artificial Neural Networks have also been employed to assess the stability of rock slopes under steady state seepage conditions, highlighting the significant influence of pore water pressure on safety factors (**Millán & Galindo, 2025**). In addition, the use of genetic programming and conceptual modelling has been recommended as a promising approach to further enhance seepage prediction capabilities (**Sharghi et al., 2018**). Comparative analyses have shown that seepage lines and discharge rates obtained from physical, mathematical, and numerical models generally agree with those from Casagrande's equations and SEEP/W software. However, the SEEP/W model performs poorly in accurately quantifying flow volume when the seepage line intersects the downstream slope (**Al-Janabi et al., 2025**). For earth-core rockfill dams, both two-dimensional (2D) and three-dimensional (3D) finite element seepage analyses are essential for accuracy. 3D analyses have demonstrated that the steady-state hydraulic gradient at the downstream toe can be nearly four times greater than the corresponding 2D value, and total discharge rates can be almost twice as high. Such differences are especially pronounced in narrow-valley settings, where reliance on 2D models alone may result in the underestimation of exit gradients and uplift forces (**Ahmed & Bazaraa, 2009; Soleimanbeigi & Jafarzadeh, 2008**). Among the many parameters influencing such analyses, hydraulic conductivity remains the most critical, directly controlling seepage quantity and pressure distribution.

Hydraulic conductivity, a critical parameter in all seepage studies, is typically assessed via Lugeon or pumping tests (**Kaleris & Ziogas, 2020**). Recent research on deep rock masses has also highlighted the significant impact of thermal conditions, revealing a nonlinear positive correlation between hydraulic conductivity and water temperature; specifically, experimental results indicate that owing to changes in fluid kinematic viscosity, the hydraulic conductivity at 80°C is 2.31 times higher than at 30°C (**Qiu et al., 2025**). Anisotropic hydraulic conductivity can increase seepage rates and reduce slope stability, especially under rapid drawdown, where the stability coefficient initially falls sharply and then stabilises as permeability increases (**Huang et al., 2017; Shuhaib & Khassa, 2024**). Among advanced modelling tools, FEFLOW 3D has proven highly effective for simulating water flow through saturated, partially saturated, and unsaturated porous media under isotropic or anisotropic conditions, using finite element and finite volume schemes based on Darcy's and Richards' equations (**Trefry & Muffels, 2007; Widomski et al., 2013a; Widomski et al. 2013b; Zhao et al., 2005**). Such analyses are vital to ensure that hydraulic structures including gravity dams, diversion dams, and stilling basins are designed to resist uplift forces and high exit gradients (**Salmasi et al., 2020**). The application of these principles is exemplified by the Karkheh Dam case, where seepage control has been a decisive factor in ensuring long-term structural safety.

Despite extensive research on seepage analysis and dam safety, few studies have integrated three-dimensional numerical modelling calibrated with in-situ measurements to quantify both maximum average hydraulic gradient and uplift pressure for large earth-fill dams under extreme flood conditions in complex geological settings. This knowledge gap is particularly critical in the case of the Karkheh Dam, where the sheer scale of the structure, complex geological setting, and history of high seepage rates make it a prime candidate for such an integrated 3D, field-calibrated analysis.

The Karkheh Dam, located in Khuzestan Province, is a large earth-fill structure with a height of 127 m and a reservoir capacity of 5.9 billion m³ at normal water level. It incorporates a 400 MW hydroelectric plant and a 110 m-wide gated chute spillway (**Heidarzadeh et al., 2019**). Following initial impoundment, high seepage rates were recorded, prompting the design and staged construction of cut-off walls extending to impervious mudstones, with the aim of reducing maximum average hydraulic gradients. Since flow through the abutments and foundation can significantly affect stability and safety (**Ahmed & Bazaraa, 2009**), this study aims to determine the hydraulic conductivity of conglomerate layers and manage seepage flux and maximum average hydraulic gradient within allowable limits. FEFLOW models, developed to account for the dam's large scale and complex geometry, used a three-dimensional domain of approximately 4.2 × 3.5 km for each abutment to capture the variable longitudinal and vertical extents of the cut-off wall and the complex seepage dynamics through existing gullies.

The applicability of this three-dimensional model is substantiated by its successful calibration against monitored seepage discharges and its validation using observation well data, confirming its capability to accurately represent the complex heterogeneous geology of the foundation. Distinct from conventional studies that predominantly focus on internal erosion and seepage within the dam embankment, this research specifically addresses the seepage through the foundation and abutments. Beyond standard validation, the application of the model proves particularly critical during extreme flood events, such as the 2019 flood, when the water level rose approximately 5 m above the normal level. By identifying the precise locations of maximum uplift pressure, specifically beneath the spillway chute, and determining the reservoir elevation at which hydraulic gradients exceed safe limits, the model serves as an essential predictive tool. This capability not only facilitates the selection of appropriate new drainage well locations for spillway stability but also enables operators to implement targeted safety measures and proactively control internal erosion risks during future hydrological crises. Ultimately, this study provides a transferable methodological framework applicable to other large dams where seepage through the foundation and abutments poses a primary stability concern.

2. Theoretical background

The governing partial differential equation describing seepage through porous media is presented in **Equation 1**. This equation combines the continuity equation with Darcy's law, yielding Richards' equation for variably saturated flow conditions. It provides an accurate representation of flow within a homogeneous, anisotropic, saturated, and incompressible porous medium. This equation was selected as it provides an accurate and standard framework for modelling steady-state seepage through saturated, anisotropic porous media, which are the representative hydrogeological conditions of the dam's foundation and abutments in our study. The finite element formulation, derived via the Galerkin method based on the principle of weighted residuals, is expressed in **Equation 2** (**Soleimanbeigi & Jafarzadeh, 2008**).

$$\frac{\partial}{\partial x}\left(\rho k_x \frac{\partial h}{\partial x}\right) + \frac{\partial}{\partial y}\left(\rho k_y \frac{\partial h}{\partial y}\right) + \frac{\partial}{\partial z}\left(\rho k_z \frac{\partial h}{\partial z}\right) = 0 \quad (1)$$

Where:

h – total hydraulic head (m),
k_x, k_y *and* k_z – hydraulic conductivities in the x, y and z-directions (*m/s*),
ρ – density of water (*kg/m³*).

$$\int_v ([B]^T[C][B])dV\,\{H\} = \int_A (q\langle N\rangle^T)\,dA \quad (2)$$

Where:

$[B]$ – gradient matrix (*1/m*),
$[C]$ – element hydraulic conductivity matrix (*m/s*),
{H} – vector of nodal hydraulic heads (*m),*
A – area of the element face (m^2),
<*N*> – represents the vector of interpolation functions (dimensionless),
q – unit flux across the element face (*m/s*).

3. Geological Characteristics and Investigations

The Karkheh Dam, completed on March 24, 2001, is founded on a geological sequence comprising conglomerate and mudstone strata. The conglomerate units display a wide range of textural characteristics, from loosely packed to densely cemented matrices. Interbedded horizontal mudstone layers act as hydraulic barriers, compartmentalizing the conglomerate into discrete aquifer units, each with distinct hydrogeological behaviour. Due to their very low hydraulic conductivity, these mudstones effectively restrict interlayer flow. As shown in **Figure 1**, the right abutment contains three mudstone horizons above the river level, designated Mud (+3), Mud (+2), and Mud (+1), and three below, designated Mud (−1), Mud (−2), and Mud (−3). Mud (+1) is considered hydraulically insignificant owing to its limited thickness and lateral discontinuity. On the left abutment, three mudstone horizons occur above the river level, numbered Mud (+2) to Mud (+4). The geological cross-section in **Figure 1** illustrates the spatial variation and elevation of these horizons. Given their distinct hydromechanical properties, the conglomerate units bounded by each mudstone layer can be individually represented in the numerical seepage models for both the right and

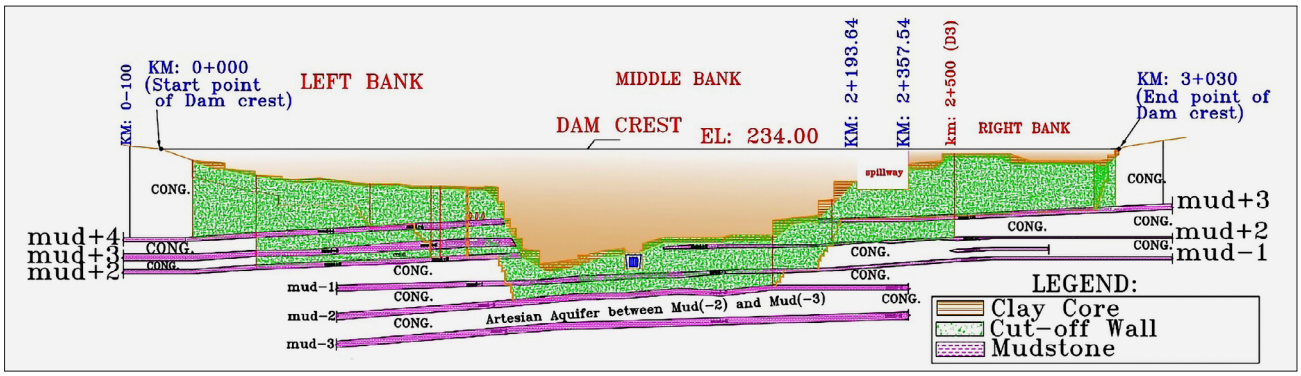


Figure 1: Longitudinal section of the Karkheh Dam foundation showing cut-off wall configuration and stratigraphic sequence across the left abutment, right abutment, and central core zones

left banks. The lateral boundaries of each model domain are defined by the mapped outcrops of the corresponding mudstone layer at the reservoir margin and on the downstream side as shown in **Figure 2** (labelled as Mud+3, Mud+2, etc.). Consequently, the respective conglomerate units receive reservoir recharge from different distances relative to the dam axis and from specific impounded areas.

It is worth noting that in **Figure 2**, the observation wells are indicated with the prefixes AW and NAW. The hydraulic heads from these wells are used to evaluate the model and compare it with real field data in subsequent sections.

Building on the identified stratigraphic configuration and its representation in the numerical seepage models, subsequent in-situ investigations were conducted to quantify the hydraulic conductivity parameters governing foundation and abutment seepage behaviour.

To determine the hydraulic conductivity of the dam foundation and abutments, a total of 823 Lugeon tests were conducted across various locations and geological strata within the foundation. These tests revealed a highly heterogeneous rock mass ranging from permeable to highly permeable. 'Open-framework' conglomerates constitute 2–3% of the highly permeable zones. Approximately 20% of the rock mass consists of conglomerate with a sandy matrix and weak cementation with Lugeon values greater than 60, extending to a depth of 30 m. Another 7% comprises conglomerate with a sandy matrix and weak-to-moderate cementation (Lugeon values of ~60). About 28% of the rock mass exhibits average Lugeon values of 30, consisting of conglomerates with either good cementation or silty-sandy matrices. Furthermore, 28% of the rock mass is composed of conglomerate with a silty matrix and weak cementation, showing an average Lugeon value of 10. Additionally, pumping tests performed in two conglomerate aquifers beneath the riverbed, specifically between mudstone layers Mud (−1) and Mud (−2) as well as Mud (−2) and Mud (−3), were used as reference values for the initial hydraulic conductivity in the seepage calibration. Pumping test results indicated hydraulic conductivity values ranging from 3.95×10^{-4} to 7.32×10^{-4} m/s. These values are approximately two orders of magnitude higher than the equivalent hydraulic conductivity estimated from Lugeon tests. This significant discrepancy is attributed to the scale effect; while Lugeon tests measure localised hydraulic conductivity, pumping tests capture the macro-permeability of the interconnected open-framework gravels and interconnected voids, which act as preferential flow paths. The hydraulic conductivity values derived from the back-analysis of the dewatering process for the hydropower excavation were consistent with those obtained from other deterministic approaches. Based on these investigations, the average hydraulic conductivity of the conglomerate was assessed as (4–9) $\times 10^{-4}$ m/s (**Mirghasemi & Pakzad, 2005**). This relatively high hydraulic conductivity is attributed to the presence of discontinuity zones and open-framework gravels within the conglomerate strata, allowing for turbulent flow. The hydraulic conductivity of the horizontally bedded mudstone layers ranged from 10^{-7} to 10^{-10} m/s, while the hydraulic conductivity of the Karkheh Dam cut-off wall was approximately 5×10^{-10} m/s (**Mirghasemi et al., 2005**).

Building upon the quantified hydraulic conductivity characteristics of the Karkheh Dam foundation and abutments, the ensuing evaluation incorporated hydraulic-gradient considerations to establish the critical threshold for internal erosion control and to inform the design length of the cut-off wall.

Experimental tests were conducted on Rhine River conglomerates, which exhibited a texture similar to that of the conglomerates in the Karkheh River. According to a technical meeting memorandum in Germany, the maximum average allowable hydraulic gradient for mitigating erosion risk in the Karkheh Dam foundation and abutments was determined to be 0.075 (**Heidarzadeh et al., 2019**). The design length of the cut-off wall was based on this critical hydraulic gradient. Following the establishment of this criterion, supplementary embankment earth fill was strategically placed in Zones 1 to 5 (see **Figure 2**) on the upstream side, as well as within the downstream gullies along the right bank. In addition

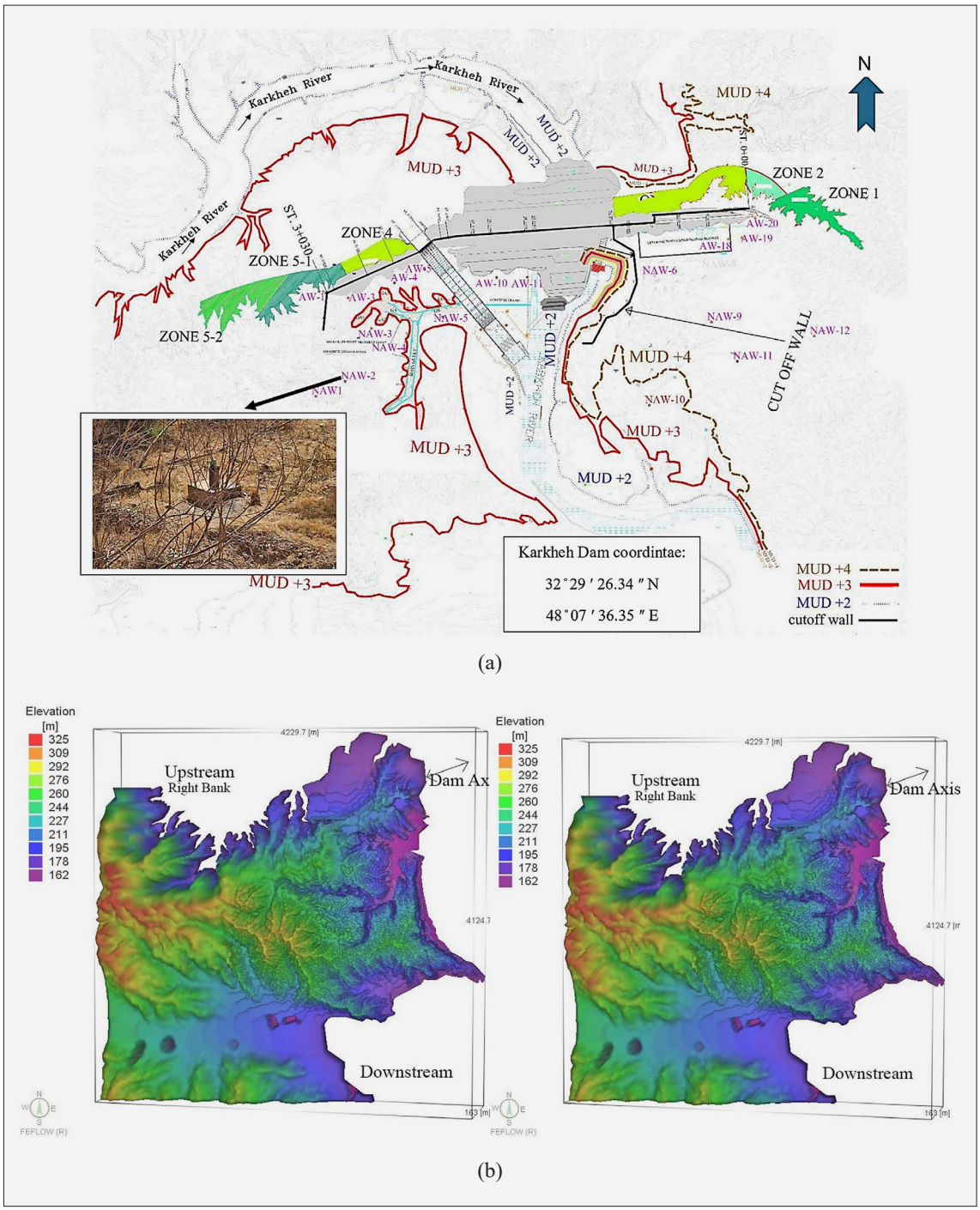


Figure 2: (a) General layout of Karkheh Dam indicating mudstone layer distributions, earthfill zones, and observation well locations. (b) Ground surface elevations (m.a.s.l.) from the FEFLOW model.

to increasing the seepage path length, these measures prevented shoreline erosion caused by wave action. During the early years of reservoir impoundment, fluctuations in water level, combined with the weak cementation of the Karkheh conglomerate, led to severe shoreline erosion (see **Figure 3a**). To address this, upstream embankments were constructed and the reservoir banks were armoured with riprap to ensure long-term erosion protection (see **Figure 3b**). Furthermore, a localised embankment was constructed to prevent water infiltration into the gully adjacent to the left abutment and to reduce seepage in Zone 1.

4. Methodology

As previously noted, the large geometry of the structure, the complex geotechnical conditions (including the longitudinal and vertical extents of the cut-off wall in the dam design, as well as seepage dynamics through existing gullies), and the relatively high hydraulic conductiv-



Figure 3: (a) shoreline erosion caused by wave action; (b) soil-cement and supplementary embankment earth fill

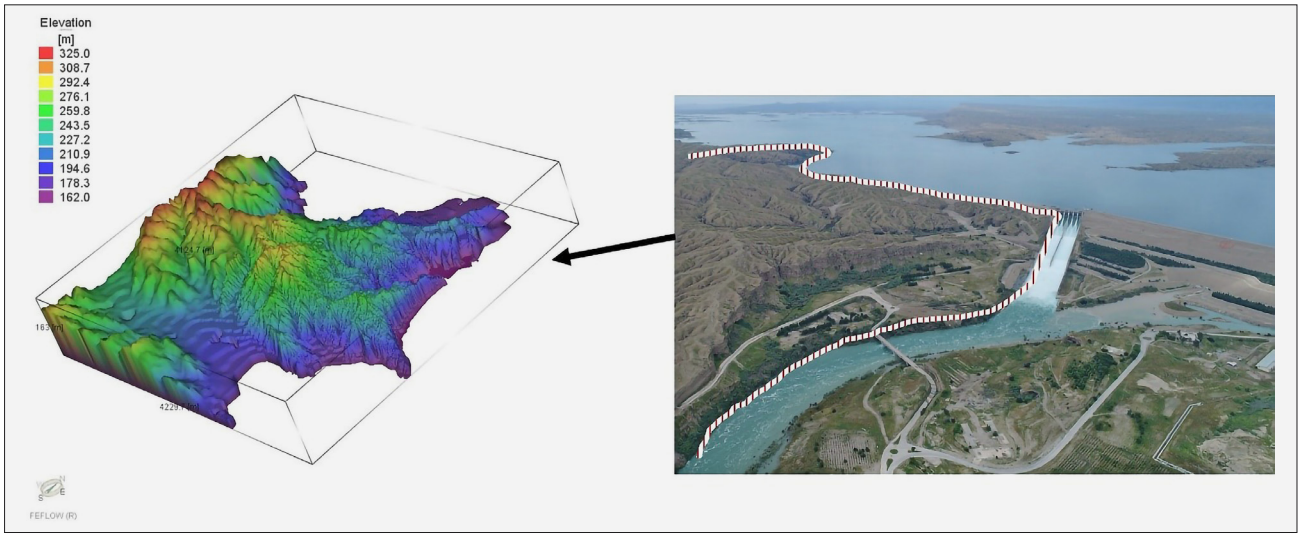


Figure 4: (a) numerical model geometry and (b) actual extent of the conglomerate above mudstone (+3) layer on the right abutment of the Karkheh Dam

ity of the foundation and abutments of the Karkheh Dam collectively necessitate a comprehensive three-dimensional seepage analysis. Given the necessity for three-dimensional analyses in such cases, FEFLOW is particularly well suited owing to its ability to model large-scale geometries, its computational efficiency, and its effectiveness in representing complex configurations. As an example of this modelling, **Figure 4a** presents the geometry of the numerical model for the conglomerate layer located above Mud (+3) on the right abutment, while **Figure 4b** illustrates the Karkheh Dam during the March 2019 flood and indicates the approximate extent of this layer.

4.1. Numerical Simulation

Considering the characteristics of the Karkheh Dam, together with the respective capabilities and limitations of state-of-the-art modelling tools, FEFLOW 3D was identified as the optimal choice for simulating seepage in geometrically complex configurations such as those present in the Karkheh Dam.

The software integrates a graphical user interface essential for the precise definition of the model geometry, with accurate delineation of boundaries being a critical step. To establish the three-dimensional model geometry, the locations of mudstone layer outcrops and the extents of the cut-off walls were initially mapped in plan view. The identification of these mudstone outcrops was achieved through the analysis of geological maps compiled during the construction phase and feasibility studies, as illustrated in **Figure 2**. By mapping the spatial distribution of each mudstone outcrop, a definitive boundary for the modelling domain was established. Earth-fill zones 1 to 5, in accordance with **Figure 2**, were also modelled. Appropriate boundary conditions were then applied to the surface topography and domain boundaries.

To ensure an accurate representation of field conditions, the thickness of conglomerate layers interbedded between mudstone strata was explicitly defined. Topographic survey data were utilized to incorporate elevation points relevant to the upper model layers. Following

planar domain definition, zones with differing hydraulic conductivity characteristics (such as cut-off walls and grout curtains) were represented using triangular prismatic three-dimensional elements. Within the inter-mudstone zones, conglomerate thickness was defined from the upper surface of the lower mudstone stratum to the base of the overlying mudstone layer.

Surface layers were modelled extending from the basal elevation of the uppermost mudstone to the specific elevations identified in the topographic survey. To finalise the three-dimensional construction, the conglomerate layer profiles, initially defined in two dimensions, were extruded to ensure volumetric continuity. The initial hydraulic conductivity parameters for these conglomerate layers were derived from the pumping test results detailed in Section 3.

It is worth noting that geologically, the dam body rests upon the upper conglomerate layers, specifically above the Mud (+3) layer in the right abutment and the Mud (+4) layer in the left abutment. However, since the primary objective of this study was to investigate seepage specifically through the foundation and abutments, the dam body itself was excluded from the simulation. Consequently, all numerical models consist solely of the foundation, abutments, and the cut-off wall, and therefore defining material properties for the earth dam body was not required.

4.2. Boundary Conditions

The upstream boundary condition was defined by the reservoir hydraulic head, applied to nodes situated below the reservoir water surface elevation. Conversely, the downstream boundary conditions were derived from comprehensive field inspections conducted during the 2019 flood events, corroborated by analyses of aerial footage and dam operational monitoring data. In fact, seepage exit elevations were determined based on site observations specific to this event. For scenarios where reservoir water levels fell below the normal operating level of 220 metres above sea level (m a.s.l.), the discharge points were adjusted proportionally to reflect these varying hydraulic conditions.

4.3. Calibration-Verification Approach and Performance Results

The model calibration process involved iterative adjustments to exit elevations and hydraulic conductivity values until the simulated seepage closely matched empirical field measurements. Hydraulic conductivity values were systematically adjusted across a range of reservoir water levels to align with site-measured discharge rates. The field monitoring program was designed to quantify seepage between individual mudstone pairs and to distinguish flow contributions from the left and right abutments through precise seepage measurements. The locations used for measuring seepage from the foundation and abutments are presented in **Figure 5**. The coloured regions delineate distinct seepage measurement zones, while the labels within the white circles correspond to the on-site identification codes for each zone. To keep the paper concise, the UTM coordinates and names of these points have been omitted.

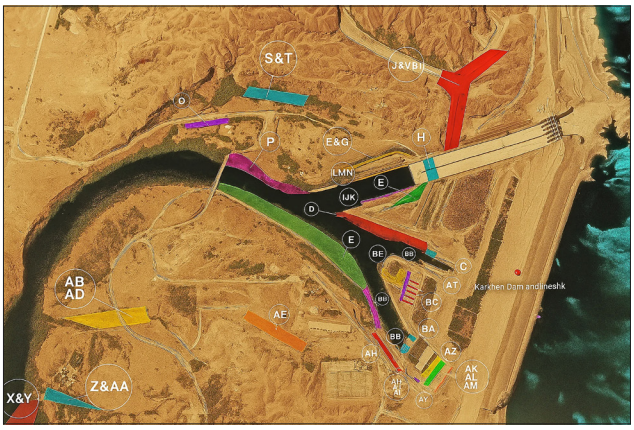


Figure 5: Location of the seepage measurement stations at the Karkheh Dam, monitoring discharge from the foundation and abutments.

Although the calibration methodology relied on a trial and error approach, which may limit precision compared with optimisation algorithms, it nevertheless provided a validated and practical framework for engineering applications. To ensure rigorous validation, hydraulic heads simulated at observation well locations were compared against field measurements from the dam abutments. Hydraulic gradients were calculated based on the differential between the reservoir water surface elevation and the hydraulic heads at the downstream exit points. Flow path lengths were determined via numerical analysis, enabling the comparison of calculated gradients with the allowable design limits. Consequently, the potential for internal erosion was evaluated across a range of reservoir water surface elevations. Furthermore, a representative average hydraulic conductivity was determined to support the estimation of total seepage discharge through the foundation and abutments. Finally, a sensitivity analysis was conducted to assess the influence of hydraulic conductivity anisotropy on the simulation results.

5. Results and Discussion

As described in the previous section, a three-dimensional (3D) seepage analysis was performed on six distinct geometries incorporating varying mudstone layers. These models were precisely matched to the actual site topography to ensure high accuracy and reliability. The hydrogeological domains were represented as representative homogeneous media, a standard simplification in deterministic seepage modelling. Although advanced probabilistic methods can account for spatial variability

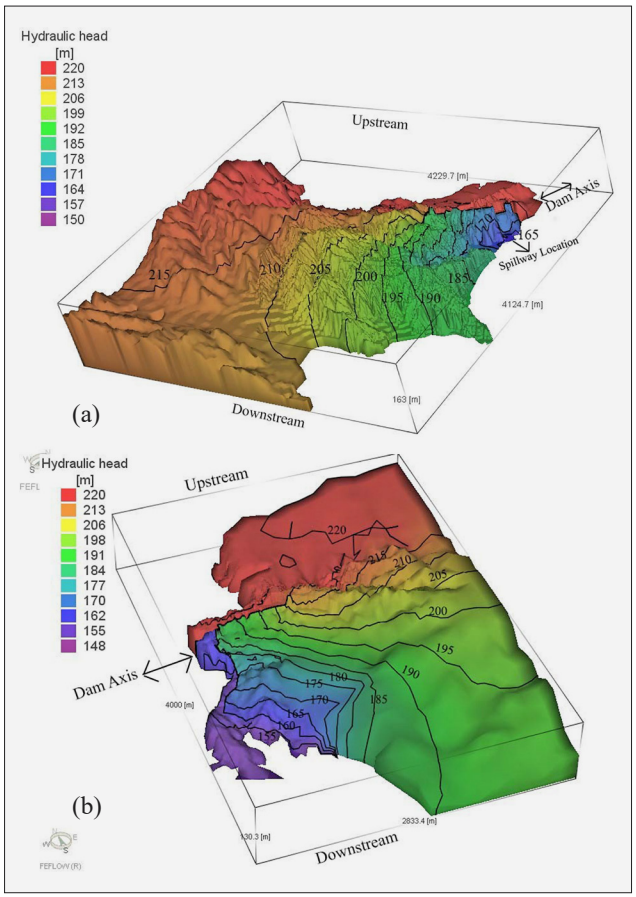


Figure 6. Three-dimensional seepage model showing equipotential lines from the numerical analysis of conglomerate layers at the normal reservoir water level: (a) Right abutment above Mudstone (+3); (b) Left abutment above Mudstone (+4).

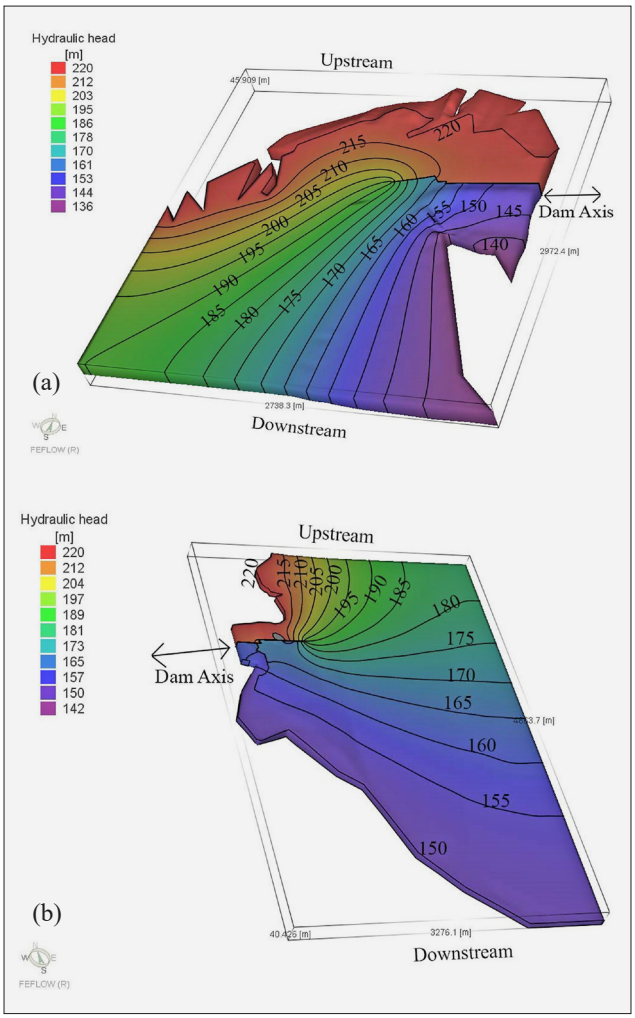


Figure 7: Three-dimensional seepage model showing equipotential lines within conglomerate layers at normal reservoir water level: (a) right abutment between mudstones (+2) and (+3); (b) left abutment between mudstones (+3) and (+4).

to assess internal erosion risks in greater detail (**Chi et al., 2025**), future research could yield more precise outcomes by conducting extensive in-situ permeability tests to capture the heterogeneity of different zones within the foundation and abutments, as well as by extending the analysis to include transient seepage modelling. The 3D models developed for the different conglomerate units, together with the associated equipotential line distributions, are presented in **Figure 6-8**. Given that the dam body was not modelled, the dam axis is shown in these figures solely to represent the schematic location of the dam and the underlying cut-off wall. The numerical simulations were calibrated for reservoir water levels of 205, 210, 220 (NWL), and 225 m above sea level. Model validation was carried out by comparing the computed hydraulic heads at the observation wells with the corresponding field measurements at the dam site. The results of this comparison for the observation wells under normal water level conditions are provided in **Table 1**.

The quantitative comparison between the numerically computed hydraulic heads and the in-situ field measurements yields a Root Mean Square Error (RMSE) of 9 m. While this value indicates some numerical discrepancies, it is widely considered an acceptable level of accuracy for validating the model's performance in complex hydrogeological studies. This conclusion is particularly valid when viewed relative to the significant total hydraulic head drop across the structure, where the error represents a relatively minor fraction of the overall hydraulic gradient. The observed discrepancies can be comprehensively attributed to three primary factors. First, a temporal mismatch existed during the monitoring period; the hydraulic head measurements did not always coincide precisely with the specific dates when the reservoir attained the simulation water levels. A typical time lag of approximately two to three days occurred before or after the target date. Moreover, the hydraulic response time of observation wells at different locations varies; not all observation points react simultaneously to a specific change in the reservoir head. Second, inherent heterogeneity within the rock mass is undoubtedly present in both horizontal and vertical profiles, creating a complex anisotropic system. Considering the extensive

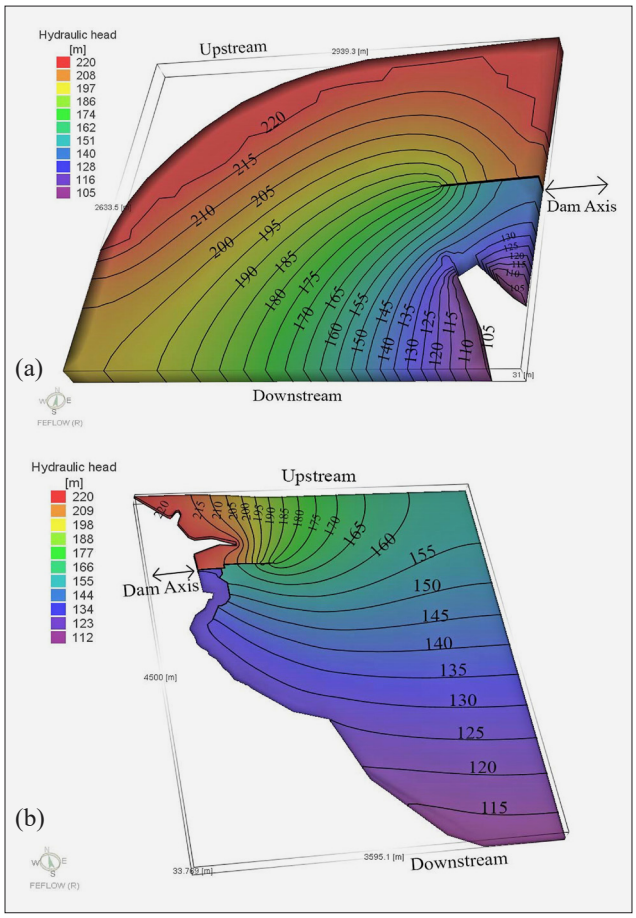


Figure 8: Three-dimensional seepage model showing equipotential lines within conglomerate layers at normal reservoir water level: (a) right abutment between mudstones (-1) and (+2); (b) left abutment between mudstones (+2) and (+3).

spatial scale of the modelled domain (spanning approximately 4 km), the necessary simplification of assuming homogeneity across such a vast domain naturally contributes to the observed deviations between the uniform numerical simulations and the spatially variable in-situ measurements. Third, and fundamentally, the numerical simulation utilizes an Equivalent Porous Media (EPM) approach to represent the fractured rock mass. Recent research highlights that the orientation of high-permeability discontinuities fundamentally dictates the flow regime, acting as the main channels for fluid movement which creates concentrated flow paths distinct from the surrounding matrix (**Namdari et al., 2021**). Since the actual groundwater flow occurs through discrete fracture networks and specific conductive features, local channelling effects can cause point-specific measurements to differ from the volume-averaged hydraulic heads calculated by the continuum model.

The Karkheh Dam spillway has a total length of 995 m, extending from the ogee to the end of the stilling basin. At the right bank, it intersects mudstone layers −1, +2, and +3 at various elevations. Numerical analysis results illustrate the variation in uplift pressure beneath the concrete slab specifically from the ogee crest to the inlet of the stilling basin (see **Figure 9**). Uplift pressure is highest at the right bank section, particularly within the conglomerate units between mudstone layers −1 and +2, and above layer +3, where it reaches up to 65 kPa. This increase in uplift pressure, exceeding values recorded during initial operation, is attributed to the clogging of drainage wells located beneath the spillway chute slab. Mitigation involves rehabilitating existing drainage wells and installing additional drainage boreholes where

Table 1: Comparison of measured and numerically simulated total hydraulic heads in observation wells at normal reservoir water level

Observation well Locating at right bank	Water Total Head (m)		Observation well Locating at left bank	Water Total Head (m)	
	Measured	Numerical Analysis		Measured	Numerical Analysis
AW6-2	216.34	215.06	AW16-1	186.48	182.6
AW3-2	184.31	188.36	AW17-1	193	188.39
AW4-2	176.89	176.81	AW18-2	200.63	194.36
AW5-2	161.76	161.55	AW19-1	205.35	200.85
NAW5-1	145.16	149.75	AW20-1	211.96	205.08
AW1-1	215.00	217.12	NAW7-1	175.38	167.47
AW3-1	186.52	177.38	NAW11-1	176	174.02
AW6-1	211.08	192.84	AW16-2	171.68	171.93
NAW2-1	189.41	186.47	AW17-2	174.94	171.21
NAW17-1	170.17	162.92	AW18-1	181.36	198
AW3-3	183.35	170.84	AW19-2	182	170.09
AW10-2	146.67	131.02	AW20-0	186.36	205
NAW16-2	139.14	141.4	NAW14-3	151.75	162.7
NAW17-2	172.56	155.31	NAW8-2	151.99	163.7
NAW5-2	151.54	145.93	NAW7-3	149.16	144.85

*Note: The Root Mean Square Error (RMSE) between the measured and numerical analysis values is 9 m.

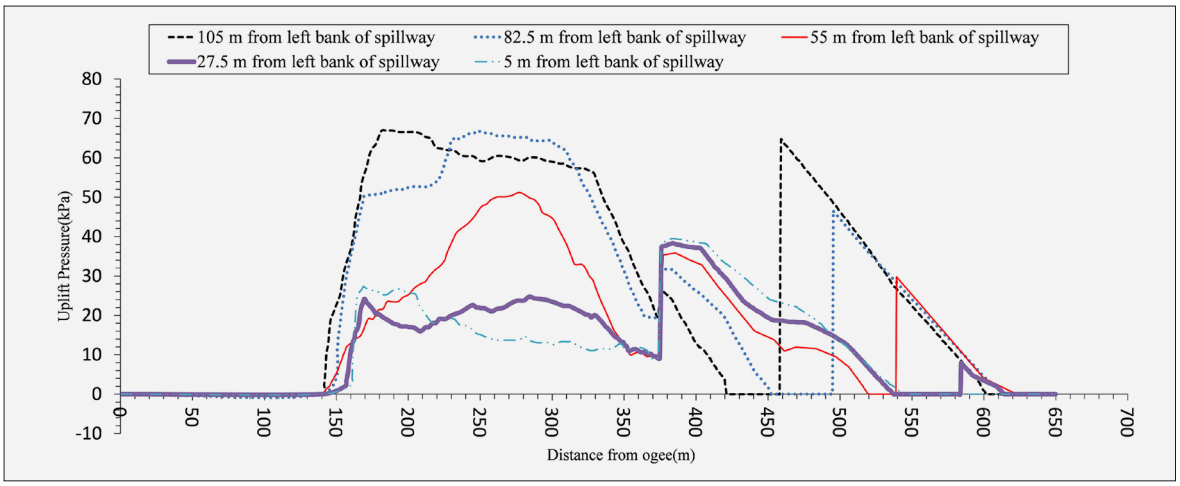


Figure 9: Evolution of uplift pressure beneath the spillway concrete slab with distance from the ogee crest at normal water level, based on five longitudinal cross-sections across the 118 m wide spillway

Table 2: Maximum average hydraulic gradients in conglomerate layers at different reservoir water levels, based on numerical analyses

Location of Conglomerate Layer	Reservoir Water Level (m.a.s.l)			
	205	210	220 (NWL)	225
Between mud (-1,+2) at the right bank	0.054	0.061	0.066	0.071
Between mud (+2,+3) at the right bank	0.056	0.066	0.069	0.076
Above mud (+3) at the right bank	0.030	0.034	0.044	0.052
Between mud (+2,+3) at the left bank	0.052	0.056	0.060	0.063
Between mud (+3,+4) at the left bank	0.030	0.032	0.036	0.040
Above mud (+4) at the left bank	0.034	0.047	0.062	0.069

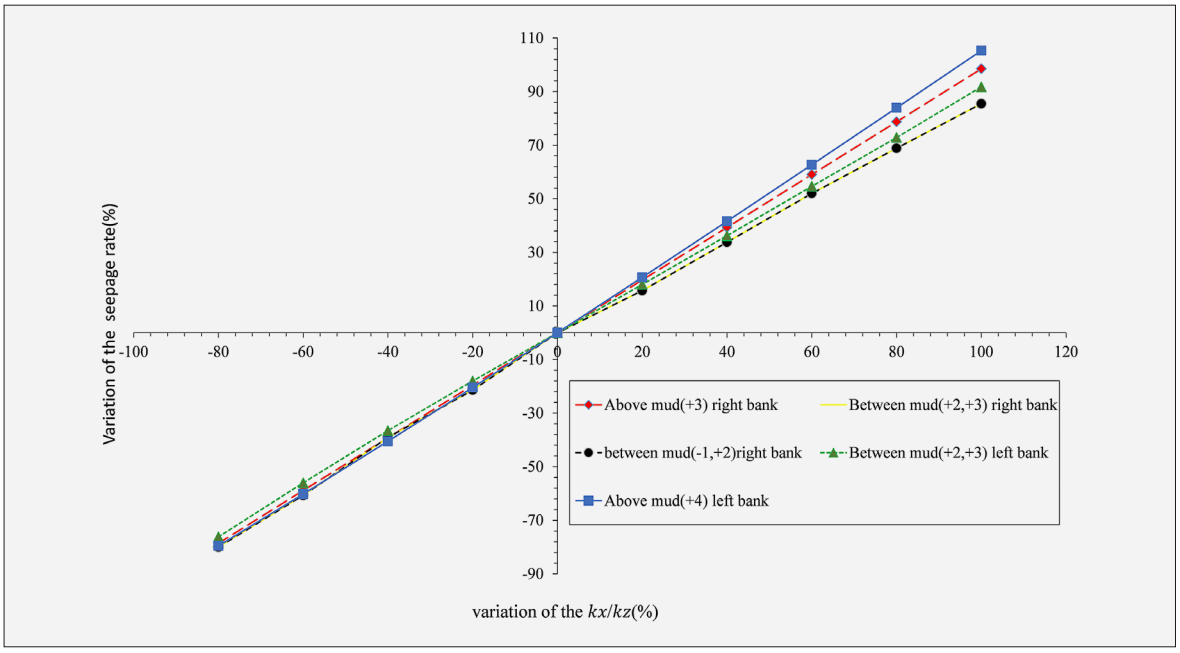


Figure 10: Sensitivity analysis of horizontal-to-vertical hydraulic conductivity ratios on seepage discharge through the Karkheh Dam abutments

uplift pressures exceed allowable limits. These works are currently in progress, with borehole locations selected based on the results of this numerical modelling. The observed reduction in uplift pressures shown in **Figure 9** is associated with the presence of intersecting low-hydraulic conductivity mudstone layers.

The average maximum hydraulic gradient, defined as the gradient along the shortest seepage streamline, for various conglomerate layers at different reservoir water levels is presented in **Table 2**, and is based on numerical analyses. The locations of maximum gradient occur within the conglomerates situated between mudstone layers +2 and +3 on the right bank, and above mudstone layer +4 on the left bank. In all examined conglomerate layers, the maximum hydraulic gradient remains below the allowable limit of 0.075, indicating that under normal reservoir conditions the gradient operates within safe limits. However, at a reservoir elevation of 225 m above sea level (m a.s.l.), the hydraulic gradient approaches the allowable limit of 0.075. Since reservoir elevations exceeding the normal operating level correspond to flood conditions where maintaining safety margins is critical (**Jain et al., 2023**), operators may temporarily store and regulate floodwater for potential use in dry periods only if strict limits are observed. Therefore, it is recommended that the reservoir level not be maintained at or above 225 m.a.s.l. to avoid establishing a steady-state seepage regime and to reduce the risk of initiating erosion in the foundation rock mass.

Following the calibration of 24 numerical analyses, an average hydraulic conductivity of 3.2×10^{-4} m/s was determined for the conglomerate layers forming the dam foundation and abutments. Using this average hydraulic conductivity in seepage calculations resulted in less than a 10 percent difference between the measured and computed seepage discharges.

During model calibration, the horizontal hydraulic conductivity was set to be ten times greater than the vertical hydraulic conductivity to achieve closer agreement with observations from well measurements. This anisotropy ratio represents a common assumption in most seepage analyses (**Bakker & Bot, 2025**). A subsequent sensitivity analysis was carried out to assess the influence of this anisotropic ratio on the dam seepage rate while keeping the horizontal hydraulic conductivity constant. In **Figure 10**, a horizontal-to-vertical permeability ratio of 5 serves as the benchmark (set as the origin at 0%, 0%), with the vertical and horizontal axes showing the percentage variations in seepage rate and anisotropy ratio, respectively. It is observed that the model sensitivity is notably higher for horizontal-to-vertical permeability ratios greater than 5. As shown in this figure, the influence of anisotropy is more pronounced in the upper conglomerate layers, where the vertical seepage component is markedly greater than in the lower layers. This vertical component is particularly significant within the outcrop zones. The results in **Figure 10** indicate that the effect of the vertical hydraulic conductivity is more pronounced in the conglomerate layers overlying the +4 mudstone layer on the left bank compared with the other cases. This aligns with recent findings indicating that the anisotropy ratio directly governs the depth of hydraulic influence; specifically, variations in pore water pressure are primarily concentrated in near-surface layers when the vertical-to-horizontal permeability ratio is low, whereas higher vertical ratios allow these pressure changes to propagate significantly into deeper zones (**Zhang et al., 2025**). Such observations underscore the critical role of vertical flow components in heterogeneous formations, consistent with reported enhancements in downward fluid migration through vertical preferential pathways (**Tafti et al., 2021**).

6. Conclusions

To examine the seepage characteristics of the Karkheh Dam foundation and its abutments, a comprehensive analysis was conducted using the Finite Element Method (FEM) in FEFLOW 3D. Three-dimensional models were developed and calibrated against empirical monitoring data, resulting in 24 distinct simulations. The study encompassed six geometrical configurations and four reservoir water levels.

The principal findings are as follows:

- The applicability of this three-dimensional model is substantiated by its successful calibration against monitored seepage discharges and its validation using piezometric data, confirming its capability to accurately represent the complex heterogeneous geology of the foundation. The application of the model is particularly critical during extreme flood events, such as the 2019 flood. By identifying the precise locations of maximum uplift pressure, specifically beneath the spillway chute, and determining the reservoir elevation at which hydraulic gradients exceed safe limits, the model serves as an essential predictive tool. This capability enables operators to implement targeted safety measures and proactively control internal erosion risks during future hydrological crises.
- The cut-off wall played a critical role in reducing the hydraulic gradient and mitigating uplift pressure. However, given the substantial cost associated with extending the wall into deeper strata, the most effective solution for controlling uplift pressure beneath the spillway slab was the installation of new drainage boreholes. Their locations, determined through three-dimensional analyses, were selected to target zones with predicted peak uplift pressures.
- The three-dimensional seepage analysis revealed that the location of maximum uplift pressure could differ from that predicted by conventional two-dimensional analysis. This finding underscores the importance of using three-dimensional modelling to accurately represent hydraulic behaviour and pressure distribution within the dam foundation and abutments, and appurtenant structures such as the spillway.

- The proposed extension of the cut-off walls was adequate for conditions corresponding to the normal reservoir water level; however, during flood seasons, water levels could exceed this threshold. Such exceedance raises concerns about the prolonged retention of surplus water for use during arid periods. The results indicate that maintaining water levels above a specified margin higher than the normal reservoir elevation for durations exceeding the time required to reach steady-state seepage presents a high risk of initiating internal erosion within the foundation rock mass.
- Sensitivity analysis of anisotropic hydraulic conductivity indicated that the best agreement with observation well data was achieved when horizontal hydraulic conductivity was one order of magnitude greater than vertical hydraulic conductivity. It is observed that the model sensitivity is notably higher for horizontal-to-vertical permeability ratios greater than 5. The impact of hydraulic conductivity anisotropy was most evident in the upper conglomerate strata, where vertical seepage components were more prominent, particularly at locations identified as potential seepage surfaces.

Acknowledgement

The authors would like to acknowledge the Mahab Ghodss Consulting Engineers for providing instrumentation data.

Funding

The authors did not receive support from any organization for the submitted work.

7. References

Ahmed, A. A., & Bazaraa, A. S. (2009). Three-dimensional analysis of seepage below and around hydraulic structures. *Journal of Hydrologic Engineering, 14*(3), 243-247. doi: https://doi.org/10.1061/(ASCE)1084-0699(2009)14:3(243)

Al-Janabi, A. M. S., Dibs, H., Sammen, S. S., Yusuf, B., Ikram, R. M. A., Alzuhairy, S. H., & Kisi, O. (2025). Comparison analysis of seepage through homogenous embankment dams using physical, mathematical and numerical models. *Arabian Journal for Science and Engineering, 50*(11), 8143-8152. doi:https://doi.org/10.1007/s13369-024-09224-x

Bakker, M., & Bot, B. (2025). The effective vertical anisotropy of layered aquifers. *Groundwater, 63*(1), 68-75. doi: https://doi.org/10.1111/gwat.13432

Chang, D. S., & Zhang, L. M. (2013). Critical hydraulic gradients of internal erosion under complex stress states. *Journal of Geotechnical and Geoenvironmental Engineering, 139*(9), 1454-1467. doi: https://doi.org/10.1061/(ASCE)GT.1943-5606.0000871

Chi, F., Carvajal, C., Peyras, L., & Breul, P. (2025). Probabilistic analysis of three different internal erosion mechanisms-Application to a real earth dam. *Engineering Geology*, 108186. doi:https://doi.org/10.1016/j.enggeo.2025.108186

Choe, Y., Choi, H., & Won, J. (2022). Suffusion of a sand–clay mixture: Impact of the ionic-concentration gradient, clay type, sand-grain size and hydraulic gradient. *Geotechnique*, 1-15. doi:https://doi.org/10.1680/jgeot.21.00335

Foster, M., Fell, R., & Spannagle, M. (2000). The statistics of embankment dam failures and accidents. *Canadian Geotechnical Journal, 37*(5), 1000-1024. doi:https://doi.org/10.1139/t00-030

Ganjalipour, K., & Fatemi Aghda, S. M. (2019). Calibration of seepage analysis sections based on observation well monitoring data: a case study on Darian dam abutments–Kermanshah province, Iran. *Modeling Earth Systems and Environment, 5*, 159-173. doi:https://doi.org/10.1007/s40808-018-0525-y

Heidarzadeh, M., Mirghasemi, A. A., Niroomand, H., & Eslamin, F. (2019). Construction and performance of the Karkheh dam complementary cut-off wall: an innovative engineering solution. *International Journal of Civil Engineering, 17*, 859-869. doi:https://doi.org/10.1007/s40999-018-0370-4

Huang, F., Luo, X., & Liu, W. (2017). Stability analysis of hydrodynamic pressure landslides with different permeability coefficients affected by reservoir water level fluctuations and rainstorms. *Water, 9*(7), 450. doi:https://doi.org/10.3390/w9070450

Jain, S. K., Shilpa, L., Rani, D., & Sudheer, K. (2023). State-of-the-art review: Operation of multi-purpose reservoirs during flood season. *Journal of Hydrology, 618*, 129165. doi:https://doi.org/10.1016/j.jhydrol.2023.129165

Kaleris, V. K., & Ziogas, A. I. (2020). Using electrical resistivity logs and short duration pumping tests to estimate hydraulic conductivity profiles. *Journal of Hydrology, 590*, 125277. doi:https://doi.org/10.1016/j.jhydrol.2020.125277

Millán, M., & Galindo, R. (2025). Stability analysis of a homogeneous rock slope under steady-state seepage using artificial neural networks. *Engineering Applications of Artificial Intelligence, 159*, 111556. doi:https://doi.org/10.1016/j.engappai.2025.111556

Mirghasemi, A., & Pakzad, M. (2005). *Uncertainty in Karkheh dam foundation permeability.* Paper presented at the Proceedings of the 73rd annual meeting of international commission On Large Dams (ICOLD).

Mirghasemi, A., Pakzad, M., & Shadravan, B. (2005). The world's largest cutoff wall at Karkheh dam. *International Journal on Hydropower & Dams, 12*(2), 90-94.

Namdari, S., Baghbanan, A., & Hashemolhosseini, H. (2021). Investigation of the effect of the discontinuity direction on fluid flow in porous rock masses on a large-scale using hybrid FVM-DFN and streamline simulation. *Rudarsko-geološko-naftni zbornik, 36*(4). doi: https://doi.org/10.17794/rgn.2021.4.5

Qiu, H., Zhu, S., Fang, H., & Lu, X. (2025). Study of Seepage Laws of Deep Rock Mass Under Different Water Tempera-

tures Based on Porous Media. *Water, 17*(3), 357. doi: https://doi.org/10.3390/w17030357

Ren, J., Shen, Z.-z., Yang, J., & Yu, C.-z. (2016). Back analysis of the 3D seepage problem and its engineering applications. *Environmental Earth Sciences, 75*, 1-8. doi: https://doi.org/10.1007/s12665-015-4837-1

Salmasi, F., Nourani, B., & Abraham, J. (2020). Investigation of the effect of the different configurations of double-cutoff walls beneath hydraulic structures on uplift forces and exit hydraulic gradients. *Journal of Hydrology, 586*, 124858. doi:https://doi.org/10.1016/j.jhydrol.2020.124858

Shahbazi, A., Saeidi, A., & Chesnaux, R. (2020). A review of existing methods used to evaluate the hydraulic conductivity of a fractured rock mass. *Engineering Geology, 265*, 105438. doi:https://doi.org/10.1016/j.enggeo.2019.105438

Sharghi, E., Nourani, V., & Behfar, N. (2018). Earthfill dam seepage analysis using ensemble artificial intelligence based modeling. *Journal of Hydroinformatics, 20*(5), 1071-1084. doi:https://doi.org/10.2166/hydro.2018.151

Shuhaib, Z. K., & Khassa, S. I. (2024). Influence of Permeability Anisotropy on Seepage and Slope Stability of an Earthen Dam During Rapid and Slow Drawdown. *Mathematical Modelling of Engineering Problems, 11*(5).

Skempton, A., & Brogan, J. (1994). Experiments on piping in sandy gravels. *Geotechnique, 44*(3), 449-460. doi:https://doi.org/10.1680/geot.1994.44.3.449

Soleimanbeigi, A., & Jafarzadeh, F. (2008). Seepage Through Rockfill Dams in Narrow Valleys *From Research to Practice in Geotechnical Engineering* (pp. 522-539).

Tafti, M. D., Ardejani, F. D., Marji, M. F., & Shiri, Y. (2021). Simulation of groundwater contamination by leakage from waste-filled mine. *Rudarsko-geološko-naftni zbornik, 36*(5). doi:https://doi.org/10.17794/rgn.2021.5.5

Trefry, M. G., & Muffels, C. (2007). FEFLOW: A finite-element ground water flow and transport modeling tool. *Groundwater, 45*(5), 525-528. doi:https://doi.org/10.1111/j.1745-6584.2007.00358.x

Widomski, M. K., Iwanek, M., Kowalski, D., & Łagód, G. (2013a). *Modeling of water flow and pollutants transport in porous media: with exemplary calculations in FEFLOW*: Politechnika Lubelska.

Widomski, M. K., Iwanek, M., & Stepniewski, W. (2013b). Implementing anisotropy ratio to modeling of water flow in layered soil. *Soil Science Society of America Journal, 77*(1), 8-18. doi:https://doi.org/10.2136/sssaj2012.0142

Xuefeng, F., Wu, Z., Lijun, L., Wen, Y., Yu, S., Zepeng, Z., & Li, Z. (2019). Analysis of sluice foundation seepage using monitoring data and numerical simulation. *Advances in Civil Engineering, 2019*(1), 2850916. doi: https://doi.org/10.1155/2019/2850916

Zhang, C., Qin, M., Hong, L., & Qi, Y. (2025). Seepage and stability analysis of fractured soil slope considering permeability anisotropy. *Scientific Reports, 15*(1), 11059. doi: https://doi.org/10.1038/s41598-025-92433-7

Zhang, D., Zhang, X., & Du, W. (2022). DEM-FEM based numerical analysis on mechanical responses of sandy soil and pipeline to seepage erosion. *Engineering Geology, 310*, 106868. doi:https://doi.org/10.1016/j.enggeo.2022.106868

Zhao, C., Wang, Y., Chen, X., & Li, B. (2005). Simulation of the effects of groundwater level on vegetation change by combining FEFLOW software. *Ecological Modelling, 187*(2-3), 341-351. doi:https://doi.org/10.1016/j.ecolmodel.2004.10.019

Zhou, C., Shen, Z., Xu, L., Sun, Y., Zhang, W., Zhang, H., & Peng, J. (2023). Global sensitivity analysis method for embankment dam slope stability considering Seepage–Stress coupling under changing reservoir water levels. *Mathematics, 11*(13), 2836. doi: https://doi.org/10.3390/math11132836

Zhou, Y., Li, C., Pang, R., Li, Y., Xu, Y., & Chen, J. (2024). A new approach for seepage parameter inversion of earth–rockfill dams based on an improved sparrow search algorithm. *Computers and Geotechnics, 167*, 106036. doi: https://doi.org/10.1016/j.compgeo.2023.106036

SAŽETAK

Trodimenzionalna analiza procjeđivanja kroz temeljne naslage brane: studija slučaja brane Karkheh

Temeljne naslage brane Karkheh sastoje se od heterogenoga geološkog profila koji čine jako propusni konglomerati isprepleteni s relativno nepropusnim muljnjacima. Nakon ekstremnih poplava u ožujku i travnju 2019. godine akumulacija je prvo dosegnula svoju normalnu razinu vode od 220 m nadmorske visine, a zatim se podigla za otprilike 5 m dosegnuvši vrhunac od 224,82 m 5. travnja 2019. godine. Iako se kruna brane nalazi na 234 m nadmorske visine, navedeni uvjeti izazvali su zabrinutost u vezi sa stabilnošću konstrukcije i potencijalnim opasnostima od procjeđivanja, osobito tijekom budućih poplava. Kako bi se umanjili ovi rizici, provedene su stroge operativne mjere radi ograničavanja hidrauličkoga gradijenta unutar dopuštenih projektnih vrijednosti, čime se smanjuje vjerojatnost unutarnje erozije i pojave procjednih kanala. Trodimenzionalni model procjeđivanja kroz temeljne naslage brane razvijen je pomoću softvera FEFLOW3D, pri čemu je obuhvaćeno šest slojeva konglomerata na četirima različitim razinama akumulacije. Model je kalibriran u odnosu na izmjereno procjeđivanje uz prilagodbu hidrauličke vodljivosti te razvijen na temelju podataka o razinama podzemne vode u piezometrima. Ključni rezultati uključivali su identifikaciju raspodjele uzgona i određivanje lokacija maksimalnoga uzgona, što je bilo ključno za planiranje novih drenažnih zdenaca. Osim toga, analizama je definirana granična nadmorska visina akumulacije iznad koje maksimalni prosječni hidraulički gradijent raste do razina koje predstavljaju povećani rizik od unutarnje erozije u temeljnim naslagama brane. Ovi rezultati, zajedno s redefiniranim parametrima propusnosti i detaljnom raspodjelom hidrauličkih gradijenata, pružaju detaljan uvid u hidrogeotehničko ponašanje brane pod ekstremnim hidrološkim opterećenjem te omogućuju ciljano upravljanje sigurnošću hidrauličkoga sustava.

Ključne riječi:
analiza procjeđivanja, brana, hidraulički gradijent, nadzor brane, FEFLOW3D

Author's contribution

Mohammad Salehinik (Ph.D. Candidate): conceptualization, visualization, writing – original draft and writing, investigation, formal analysis and software. **Ali Asghar Mirghasemi** (Professor): conceptualization, methodology, supervision, resources, validation and review & editing. **Ahmadreza Tabibnejad** (Manager of Soil/Rock Mechanics & Earth Dams Department): conceptualization, data curation, project administration, supervision, resources and validation.
All authors have read and agreed to the published version of the manuscript.